# IMPACT DAMAGE TOLERANCE OF TENSION LOADED BONDED SCARF REPAIRS TO CFRP LAMINATES

**Israel Herszberg*, Stefenie Feih**, Andrew J. Gunnion* and Henry C.H. Li****

*** Cooperative Research Centre for Advanced Composite Structures Limited**
**506 Lorimer Street, Fishermans Bend, Victoria, 3207, Australia**
**** School of Aerospace, Mechanical & Manufacturing Engineering, RMIT University, GPO Box 2476V, Melbourne, Victoria, 3001, Australia**

**Keywords: Carbon composite, bonded repair, scarf joint, impact, FEA, cohesive elements**

***Abstract***

*Adhesively bonded composite repairs are an attractive option for aircraft structures. Scarf repairs are often used where high strength recovery and/or flush surfaces are required. These are subject to the same impact risk as the parent structure and consequently, it is essential to assess their durability in the case of impact. A previous preliminary experimental study found an instance of catastrophic failure of a composite scarf joint subject to impact whilst prestrained to 3000 με. It was postulated that this phenomenon is a result of failure in the joint due to the combination of the prestrain and global structural oscillations resulting from the impact event. In this investigation, a finite element analysis replicated such catastrophic failure. The conditions of impact velocity and preload were established for which such failure is predicted to occur.*

## 1 Introduction

Bonded composite patches are often used as an economical repair strategy to restore the strength of aerospace structures subsequent to damage. This may be in the form of scarf repairs in the case where there is a requirement for a flush surface, or external patch repairs when the surface condition is not critical. Scarf repairs are commonly implemented for maximum strength recovery, with additional external overplies to improve damage tolerance, unless extreme surface flushness is required (e.g. for stealth or aerodynamic considerations). Significant cost savings may be realised compared to the alternative of component replacement.

Bonded repairs on the external surface of an aircraft are subject to the same impact risks as those of the parent structure. Consequently, an understanding of the impact response and tolerance of such repairs is essential to enable the assessment of their effectiveness and durability.

The impact resistance of polymer composite structures has been a topic of intensive investigation over many years, which has been reviewed by Abrate [1] and Ried et al. [2]. Most of the studies reported in the literature, of impact on composite structures, have been conducted with the impact taking place on unloaded structures. This however, does not truly represent events likely to be encountered in real life, such as impact by runway debris, hailstones and bird strikes. In the limited literature on the impact of prestrained composite structures, it has been reported that catastrophic failure was found to occur in cases when panels were impacted at levels which, when applied to the unloaded panels did not reduce significantly their residual strength [e.g. 3].

Preliminary results for an experimental study of impact on scarf joints, representative of scarf repairs, have been reported elsewhere [4]. In one instance in particular, it was found that catastrophic failure of the joint occurred at a prestrain of about 3000 με. It was postulated that the phenomenon of catastrophic failure due to impact on structures loaded to moderate strain levels, is not a function of local damage due to impact but it is a result of the combination of the prestrain and the global oscillations, caused by the impact, exceeding allowable strains.

To test this hypothesis a finite element analysis (FEA) was undertaken, where the adherends were modelled as homogeneous orthotropic materials and failure was allowed to occur only in the adhesive layer represented by a cohesive material degradation model.

This paper summarises the previous experimental results and presents results from the FEA which predicts the occurrence of catastrophic failure under particular loading and impact conditions.

## 2 Experimental Study

Impact tests were conducted on plain composite panels and panels incorporating a 5° full-width scarf joint in their middle. The tests were conducted at various specimen preloads to produce prestrains ranging from 0 to 3000 με (nominal). The specimens, supported only in the grips of the test-rig, were impacted at their centre point with a impact energies up to 17 J. A schematic of the scarf joint test specimen is shown in Figure 1.

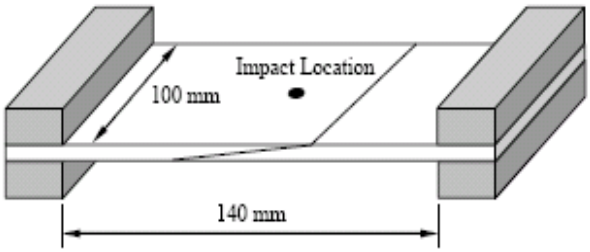


Fig. 1. Schematic of scarf joint specimen installed in friction grips

A quasi-isotropic carbon/epoxy panel was used as the subject of this study. The material used was the Cycom T300/970 prepreg system with a ply thickness of 0.2 mm. The 16-ply lay-up sequence was $[45\ 90\ -45\ 0]_{2s}$ which yielded a nominal panel thickness of 3.2 mm. The dimensions of the test panels were 100 mm wide by 200 mm long. Both plain panels and scarf joint specimens were prepared. The scarf joint specimens were machined to produce a 5° scarf which was bonded using FM73 film adhesive with a nominal thickness of 0.38 mm, cured at 120°C for 2 hours under a vacuum bag.

Impact testing was conducted under a tensile preload applied to the test specimens along the length direction via friction grips, each extending over 30 mm of the specimen length. The specimens were supported only at the grips leaving an unsupported region of 100 mm by 140 mm. The specimens were impacted at their centre with an impactor of mass 305 g with a 12 mm spherical tup. Impact energies up to 17 J were employed, with a corresponding incident momentum of 3.35 kg m/s. The tensile preload varied so as to produce a maximum strain of 3000 με.

Preliminary results showed that catastrophic failure may occur during impact under some conditions. One specimen failed catastrophically at a prestrain of 3000 με at an incident momentum of 2.62 kg m/s, while a second specimen when impacted at the same prestrain with a velocity of 2.80 kg m/s suffered only minor local damage. Further tests are being conducted to experimentally explore the conditions of prestrain and impact velocity leading to catastrophic failure.

## 3 Catastrophic Failure Hypothesis

It is postulated that two events occur as a result of impact, which are only weakly related.

The first, which is not expected to cause catastrophic failure for the range of prestrains considered in this investigation, involves local crushing and delamination resulting from through thickness strains caused by the impact. These are related to the impact energy.

The second leads to catastrophic failure under certain conditions. The impact causes global vibration which may cause failure in the event that its amplitude is sufficiently high. This failure will occur at regions of high strain, which may be remote from the impact site and will occur subsequent to the impact, at a time interval of a quarter (or three quarters) of the period of vibration. The amplitude of such vibration is dependant on the impulse and hence the impact momentum, rather than the impact energy.

## 4 Finite Element Analysis

An advanced FEA was undertaken to test the above hypothesis and to examine the conditions of prestrain and impact velocity leading to catastrophic failure and to determine the residual strength for those conditions where catastrophic failure does not occur. To simplify the model, damage was only allowed to occur in the adhesive.

Two models were used:

- The first was a model of a standard tensile test on a scarf joint, which was used to validate the adhesive damage models against tensile tests.
- The second was a model of the impact test described above.

### 4.1 Model Details

The finite element model was created in MSC.Patran and analysed in Abaqus/Standard. The model was parameterised so that joint dimensions, boundary conditions and gripping area could be easily changed if required.

The adherends were modelled as homogeneous orthotropic materials in order to simplify the model and because a 3-D composite damage model is currently not available in Abaqus. This means that composites ply-by-ply damage cannot be observed. However, as postulated above, composite damage plays a minor role compared to the adhesive failure during impact. Catastrophic impact damage occurs by adhesive failure, and this failure mode needs to be captured accurately. Table 1 presents the orthotropic adherend properties as calculated by MSC.Patran for the $[45\ 90\ -45\ 0]_{2s}$ lay-up, based on Cycom T300/970 properties obtained from the manufacturers data sheets.

Table 1. Adherend material properties

| Material property | Value |
|---|---|
| $E_1$ [GPa] | 47.1 |
| $E_2$ [GPa] | 47.1 |
| $E_3$ [GPa] | 8.30 |
| $G_{12}$ [GPa] | 17.9 |
| $G_{13}$ [GPa] | 3.85 |
| $G_{23}$ [GPa] | 3.85 |
| $\nu_{12}$ | 0.313 |
| $\nu_{13}$ | 0.262 |
| $\nu_{23}$ | 0.262 |

This approach of using orthotropic adherends does not allow the in-plane stiffness and the bending stiffness to be simultaneously accurately modelled. The choice was made to accurately model the in-plane stiffness which led to a 50% overestimate of the bending stiffness. It was however, considered to be more important to correctly model the in-plane stiffness and so ensuring the correct modelling of the prestress in the bondline.

The adhesive layer was modelled with 8-noded Hex elements and the composite adherends were modelled with 6-noded Wedge elements.

### 4.2 Boundary Conditions

For the static tests, the specimen ends were gripped over a long distance and rotation of the grips was restricted. The boundary conditions were therefore modelled as fully restricted. The displacement was applied under displacement control.

For the impact tests, the boundary conditions were not as well defined. The test set-up used a hydraulic ram to apply load, with resulted in a defined prestrain, prior to impact. The prestrain was monitored with a strain gauge in the centre of the specimen, in the middle of the scarf. Realistically, this results in a force controlled boundary condition. However, due to the short time duration of the impact event, it is questionable whether the feedback system could react to adjust the force accurately. Consequently, fixed boundary conditions were applied in the model. The impactor was restrained to move in a path normal to the panel, modelling the test situation where the impactor was restrained by rails.

The model, furthermore, restricted rotation at the grips. The relatively short length of the grips would in fact allow some rotation. The extent of this rotation had not been established.

### 4.3 Adhesive Damage Models

Two failure models were considered for the Cytec FM 73 adhesive layer.

- An elastic plastic deformation model, with stiffness reduction at failure.
- A cohesive damage model.

Both models predicted identical behaviour of tensile test specimens up to first yield. Thereafter the cohesive model diverged from the test results. Nevertheless, the cohesive model was chosen for subsequent impact analyses because the elastic plastic model suffered numeric instability subsequent to the onset of adhesive failure in some regions.

#### *4.3.1 Elastic-plastic analysis*

The adhesive layer was modelled as simply elastic-plastic. Abaqus applies metal plasticity in this case with a defined von Mises yield surface.

The shear and tensile properties of Cytec FM 73 adhesive in adhesively bonded joints have been experimentally determined [5,6]. The appropriate elastic-plastic properties are presented in Table 2.

Table 2. Elastic-plastic material properties for Cytec FM 73 film adhesive

| Material property | Value |
|---|---|
| $E_1$ [GPa] | 2.2 |
| $G_{12}$ [GPa] | 0.8 |
| $\sigma_{yield}$ | 32.0 |
| $\gamma_{ult}$ | 0.55 |
| $\sigma_{fail}$ | 0.32 |

The material behaves isotropically and the Von Mises yield criterion can be applied for this material in an elastic-plastic model.

To ensure failure detection of the adhesive layer, a maximum plastic strain is specified, after which the stress is reduced to 1% of the original value. Convergence problems were encountered with this approach.

### *4.3.2 Cohesive element model*

The adhesive layer was modelled with cohesive elements. This approach was used for the impact analysis because it demonstrated better convergence than the elastic-plastic model.

Eight node 3-D cohesive elements within Abaqus [7] were used to model the adhesive layer. The cohesive model material properties presented in Table 3, were derived from the published experimental data for Cytec FM 73 [5,6,8].

Table 3. Cohesive material properties for FM 73

| Material property | Value |
|---|---|
| $K_1$ [MPa] | 2200 |
| $K_2$ [MPa] | 805 |
| $K_3$ [MPa] | 805 |
| $G_I$ [N/mm] | 3.00 |
| $G_{II}$ [N/mm] | 6.50 |
| $G_{III}$ [N/mm] | 6.50 |
| $\sigma_{ult,1}$ | 55.0 |
| $\sigma_{ult,2}$ | 32.0 |
| $\sigma_{ult,3}$ | 32.0 |

### *4.3.4 Comparisons*

Two tensile tests were conducted on scarf joint specimens. These were modelled by using both the elastic-plastic model and the cohesive model for the adhesive layer. The results of these models were compared to each other and to the experimental results.

As expected, both models predict failure in shear with the shear stress being quite uniform across the adhesive layer. The peel stresses peak at the scarf edges, but rapidly fall to zero away from the edge. These peel stresses are generated by out of plane bending displacements in the region of the scarf joint. Both models yield similar results for the shear and peel stress distributions in the adhesive layer.

The experimental load displacement curves for two tension test specimens, together with those predicted using elastic plastic and cohesive models for the adhesive layer, are compared in Figure 2. The displacement for the model is derived for the same distance of 70 mm as recorded in the experiments using an extensometer spanning the scarf joint.

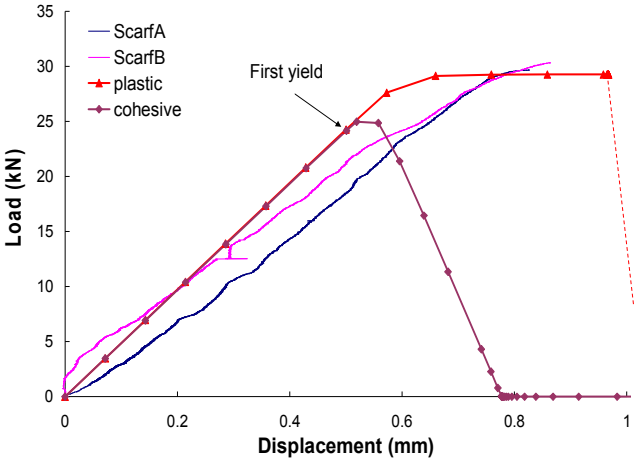


Fig. 2. Tension test load displacement curves: experimental; elastic-plastic and cohesive models

The elastic-plastic model predicts behaviour much closer to the experimental results than does the cohesive model which produces a more conservative result. Both models predict damage onset at the same displacement, however, while the elastic-plastic model can hold the same stress during yielding, the triangular shape of the cohesive model leads to an immediate drop in load carrying capacity in the yielded region which must then be taken up in the remaining unyielded adhesive. The displacement over which failure occurs is therefore far smaller than that for the elastic-plastic model. The current standard cohesive model implemented in Abaqus/Standard does not capture plastic yielding.

Notwithstanding its inferior performance, the conservative, cohesive model was used for all further impact studies because of its superior numeric stability.

### 4.4 Impacted of Scarf Joints

The impactor is modelled as a rigid body, which reduces simulation time. In order to simplify meshing it is modelled as a half hollow sphere with a diameter of 12 mm. The impactor was modelled as hollow to simplify meshing. It impacts the scarf joint normal to the surface with a specified impact velocity. The contact definition used in Abaqus for this case was surface-to-surface contact with small sliding. Impact was modelled in Abadus/Standard via the Dynamic solution.

The impactor details for the model, are presented in Table 4.

Table 4. Impactor properties for FEA

| Property | Value |
|---|---|
| Mass | 0.253 kg |
| Diameter (outer) | 12 mm |
| Diameter (inner) | 6 mm |
| Impactor deformation | None (Rigid) |
| Incident momentum | 0 – 3.8 kg m/s |

### 5 Results

The calculations followed the following three steps:

1. The panel was preloaded to one of the prestrain levels defined in Table 5 (static step).
2. For each prestrain the panel was impacted with a velocity in the range 0 - 20 m/s as shown in Table 5 (dynamic step).
3. The residual tensile strength was determined by increasing the axial displacement until failure (static step).

The test matrix and a summary of the results are presented in Table 5.

At each test point the following was determined:

- contact force history;
- damage area in the adhesive layer;
- reaction force history;
- residual reaction force;
- impactor velocity history;
- residual strength

Table 5. Selected test Matrix and Results Summary

| Pre-load [kN] | Prestrain [με] | Momentum [kg m/s] | Residual strength [kN] | Impact damage area [%] |
|---|---|---|---|---|
| 0 | 0 | 0 | 99.9 | -- |
| 0 | 0 | 5.06 | 0.0 | 100.0 |
| 9.86 | 800 | 3.16 | 73.3 | 29.1 |
| 9.86 | 800 | 3.79 | 61.8 | 41.2 |
| 9.86 | 800 | 4.43 | 0.0 | 100.0 |
| 14.8 | 1200 | 1.27 | 99.0 | 0.0 |
| 14.8 | 1200 | 12.5 | 73.6 | 29.5 |
| 14.8 | 1200 | 3.16 | 61.2 | 42.5 |
| 14.8 | 1200 | 4.43 | 0.0 | 100.0 |
| 29.6 | 2400 | 2.53 | 82.4 | 20.5 |
| 29.6 | 2400 | 3.16 | 70.1 | 32.3 |
| 29.6 | 2400 | 3.79 | 42.5 | 61.1 |
| 49.2 | 3900 | 1.89 | 91.7 | 11.5 |
| 49.2 | 3900 | 2.53 | 75.1 | 26.8 |
| 49.2 | 3900 | 3.16 | 0.0 | 100.0 |

### 5.1 Contact Force History

Figure 3 shows the influence of the prestrain on the impact force-time history for incident momentum of 3.8 kg m/s.

In the initial portion of the force-time history (A), the force increases with increases in prestrain, because of the increased stiffness of the prestrained plate.

However, in the later portion of the force-time history (B) the force decreases with increases in prestrain. This is presumably because an increased prestrain leads to an increase of the damage in the bondline, consequently causing the joint to become more compliant.

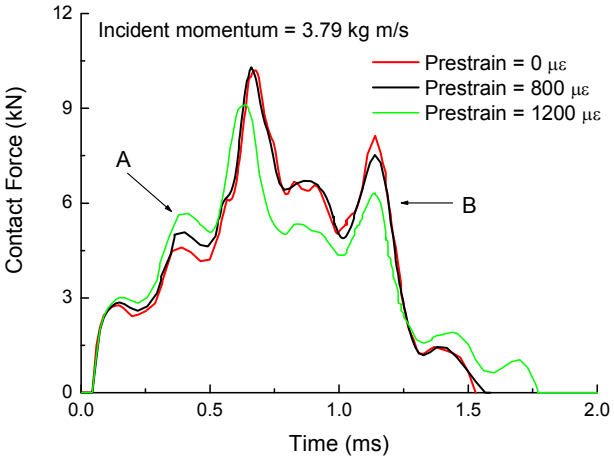


Fig.3. Contact force-time history for different prestrains and incident momentum of 3.8 kg m/s

### 5.2 Impact Damage Area

Impact damage area increases with prestrain, as may be seen from Figure 4, which shows the extent of damage in the adhesive layer as a result of impacts with an incident momentum of 3.8 kg m/s for different prestrains. A damage area is defined where the damage index exceeds 0.9, corresponding to the red and dark orange areas on the fringe plots

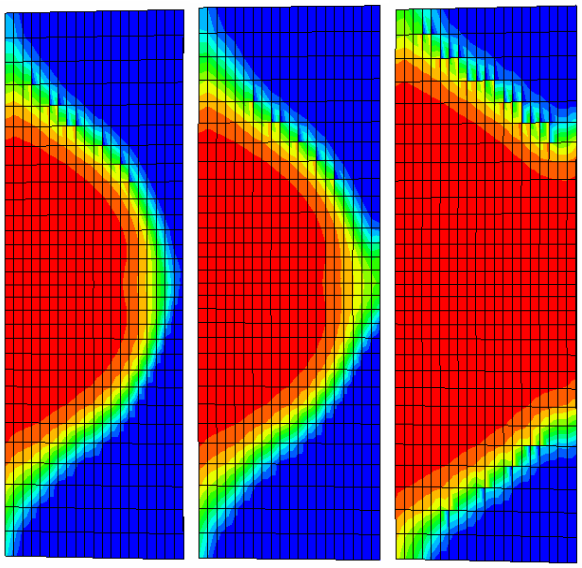

*(a) 800 με* *(b) 1200 με* *(c) 2400 με*

Fig. 4. Failure in adhesive layer at various prestrains for an incident momentum of 3.8 kg m/s. The red area corresponds to a damage index exceeding 0.92.

### 5.3 Reaction Force History

The reaction force after impact is determined by calculating the reaction forces at the displacement boundary condition. Figure 5 shows the reaction force-time history for different preloading strains. For 800 and 1200 με, the initial reaction force prior to impact is recovered. For 2400 με, a drop in reaction force is obtained due to the excessive damage of the adhesive layer. The initial force can, however, be recovered with additional loading. The specimen is therefore not considered to have failed.

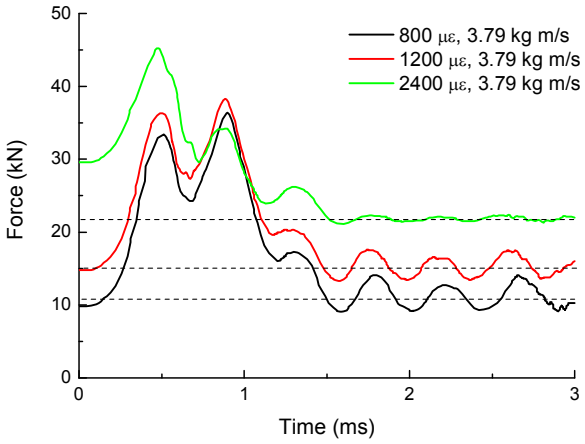


Fig. 5. Reaction force-time history for different prestrains

An example of the reaction force history for a specimen which failed catastrophically is presented in Figure 6, for a prestrain of 3800 με and an incident momentum of 3.8 kg m/s. The reaction force rapidly reduces to zero.

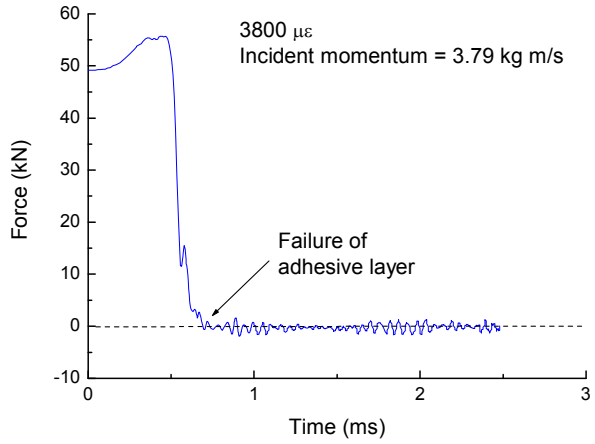


Fig 6. Reaction force history for catastrophic failure on impact.

## 5.4 Residual Strength

The residual tensile strength was determined for each damage case. Examples of the results of these calculations are presented in Figure 7. As expected, the specimens with greater damage exhibit lower stiffness and strength during subsequent loading.

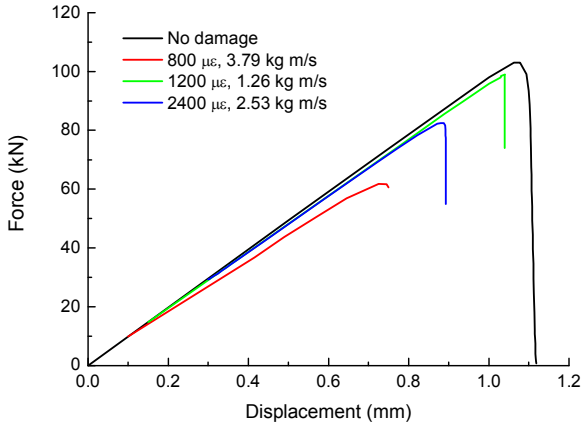


Fig. 7. Residual tensile strength for different prestrain and impact conditions

When the residual strength is plotted against damage area, it may be seen from Figure 8 that a linear plot is obtained, indicating that stress concentrations introduced by the damage as modelled have negligible effects. This result means that it is unnecessary to calculate residual strengths using the FEA.

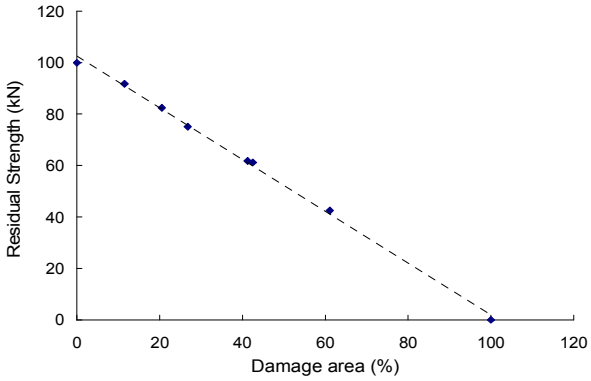


Fig. 8. Residual strength versus impact damage size

## 5.5 Summary

Results of this study are summarised in Figure 9 which shows the relationship between damage area, strength and impact velocity. For a given pre-strain, the damage area appears to increase exponentially with velocity. For example, for the highest pre-strain of 3800 με, the damage area increases from 25 - 100% by increasing the incident momentum from 2.13 - 3.16 kg m/s. The damage area is inversely proportional to residual strength as is indicated by the right hand axis in Figure 9.

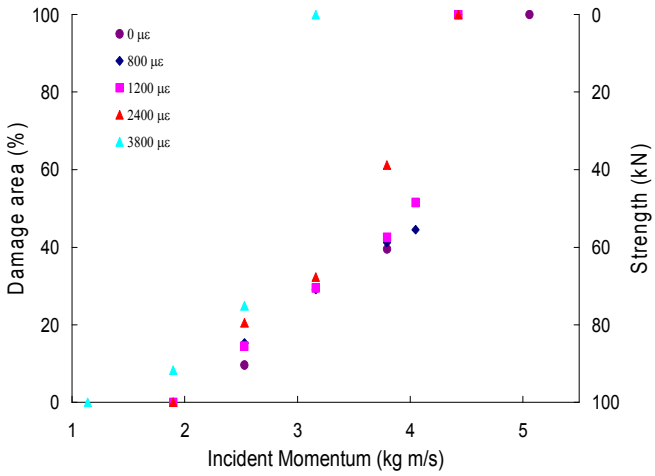


Fig. 9. Incident momentum vs. damage area and residual strength

The critical incident momentum boundary separating between local damage and catastrophic failure is plotted in Figure 10 against prestrain. It may be seen that this boundary can be approximated by a straight line.

The catastrophic failure event observed during experiments occurred at a prestain of 3000 με. at an incident momentum of 2.62 kg m/s, which compares to a value 2.9 kg m/s from Figure 10. This value would be expected to decrease if the correct bending stiffness was considered in the model. This could be accommodated by modelling the adherends ply by ply.

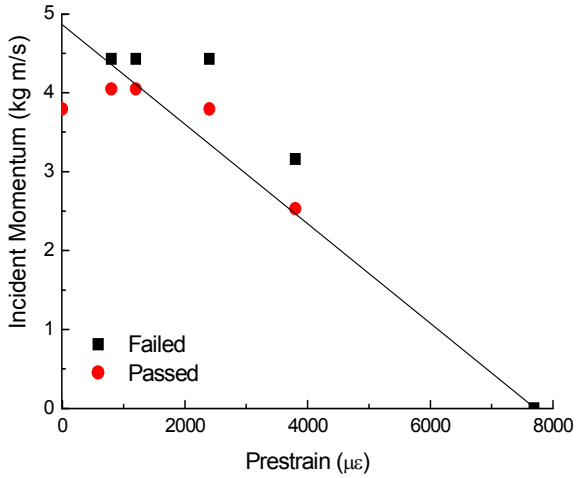


Fig. 10: Critical momentum boundary versus prestrain

## 5 Design Implications

The design of scarf repairs has hitherto been based solely on static strength requirements [8]. Consequently, the impact tolerance of such repairs has been largely neglected. However, it can be seen from the previously reported limited preliminary test results and the present FEA that the impact tolerance of the scarf joint is inferior to that of the parent structure in many cases, except when lightly loaded (1000 με prestrain). Of particular concern is the indication that catastrophic failure may occur as a result of impact at panel strain levels in the order of 3000 με which is within the normal design limit load values.

The test results and models were obtained for simple scarf joint with no surface overply. It is believed that the addition of an overply may improve the impact resistance by increasing the flexural stiffness of the repaired region and thereby reducing the adhesive stresses during impact. Naturally, further testing and modelling is required to confirm this hypothesis. If proven, this would reinforce the importance of the overply in the implementation of the scarf joint as previous shown by Gunnion et al. from the perspective of static strength [9].

It must be noted however, that the test results are relevant to monolithic composite structures only. The behaviour of fully supported sandwich structures may be significantly different due to the different support conditions. This is particularly important for the catastrophic failure case.

## 7 Conclusion

The numerical study in this report presents a first attempt at modelling the impact failure of bonded scarf joints.

It demonstrates the propensity of such joints to fail catastrophically when impacted and also simultaneously subjected to prestrains.

The method allowed the calculation of critical velocity boundaries versus prestrains.

A previously observed case of catastrophic failure in such joints occurred at velocity and prestrain which is consistent with results predicted by the model.

The numerical study furthermore shows that the damage area can be directly related to the strength of the scarf joint, which is an important observation.

It is recommended to investigate the following issues in future work:

- Influence of ply-by-ply resolution of the adherend material (will change bending stiffness)
- Influence of incorporating composite damage in ply-by-ply approach
- Advanced material model for plastic yielding and failure of adhesive (not currently available in Abaqus/Standard)

## Acknowledgement

This project is supported by *International Science Linkages* established under the Australian Government's innovation statement, *Backing Australia's Ability.*

## References

[1] Abrate, S., Impact on composite structures, Cambridge University Press, 1998.

[2] Reid, S. R. and Zhou, G. (eds), Impact behaviour of fibre-*reinforced composite materials and structures*, CRC Press, Woodhead, pp. 1-32, 2000.

[3] Herszberg I, Weller T, Leong K.H. and Bannister M., Residual tensile strength of stitched and unstitched carbon/epoxy laminates impacted under tensile load. Proc. 1st Australian Congress on Applied Mechanics, Melbourne. 21-23 February 1996.

[4] Li, H.C.H., Mitrevski, T. and Herszberg, I., Impact on bonded repairs to CFRP laminates under load, in Proc. 25th Congress of the International Council of the Aeronautical Sciences, Hamburg, Germany, 3-8 September 2006.

[5] Wang, C.H. and Chalkley, P., Plastic yielding of a film adhesive under multiaxial stress, International Journal of Adhesion and Adhesives, 20, pp. 155 – 164, 2000.

[6] Aydin, M. D. , Özel, A. and Temiz, S., Non-linear stress and failure analysis of adhesively-bonded joints subjected to a bending moment, Journal of Adhesion Science and Technology, 18 (14), pp. 1589-1602, 2004

[7] Abaqus reference manuals, Version 6.6, Abaqus Inc., 2006

[8] Baker A.A., Dutton, S. and Kelly, D.W. Composite materials for aircraft structures. AIAA Inc., Reston, USA. 2004.

[9] Gunnion A.J. and Herszberg I. Parametric study of scarf joints in composite structures. Journal of Composite Structures, in press.